Universiteit Leiden
The Netherlands

Adaptive coupling between neurons widens the entrainment range of the suprachiasmatic nucleus

Zheng, W.X.; Gu, C.G.; Yang, H.J.; Wang, H.Y.; Rohling, J.H.T.

Citation
Zheng, W. X., Gu, C. G., Yang, H. J., Wang, H. Y., & Rohling, J. H. T. (2024). Adaptive coupling between neurons widens the entrainment range of the suprachiasmatic nucleus. *Physical Review E*, *110*(3). doi:10.1103/PhysRevE.110.034212

Version:	Publisher's Version
License:	Leiden University Non-exclusive license
Downloaded from:	https://hdl.handle.net/1887/4301215

Note: To cite this publication please use the final published version (if applicable).

Adaptive coupling between neurons widens the entrainment range of the suprachiasmatic nucleus

Wenxin Zheng,[1] Changgui Gu,[1,*] Huijie Yang,[1] Haiying Wang,[1] and Jos H. T. Rohling[2]
[1]*Business School, University of Shanghai for Science and Technology, Shanghai 200093, People's Republic of China*
[2]*Department of Cell and Chemical Biology, Leiden University Medical Center, Leiden 2300RC, Netherlands*

(Received 10 April 2024; accepted 28 August 2024; published 23 September 2024)

In many realistic systems, such as neural networks in the brain, the coupling strength between neurons is not fixed, but adaptively adjusts according to their activities. The suprachiasmatic nucleus (SCN), as the main clock in the mammalian brain, has been found to be a plastic neural network, and the coupling strength between neurons is highly dynamical. An important function of the SCN is entrainment, reflecting the ability of the SCN to synchronize with the external light-dark cycle. The entrainment ability is reflected by the entrainment range, which is a period range for the external light-dark cycle to which the SCN can entrain. In this article, we investigated whether the entrainment range of the SCN is affected by the adaptive coupling. We use a modified Kuramoto model with external light-dark cycle. We found that when the light sensitivity is larger than the fixed coupling strength (the coupling strength without adaptive rules), adaptive coupling can widen the entrainment range. Our findings help to understand the impact of the adaptive coupling between oscillatorty neurons on the collective behavior of the SCN, and provides a possible explanation for the plasticity of coupling in the master clock network.

DOI: 10.1103/PhysRevE.110.034212

I. INTRODUCTION

It is well known that neurons in the brain are coupled with each other to form neural networks. The coupling strength is an important factor in studying the dynamical behaviors of these complex networks [1,2]. In many practical networks, it has been found that the coupling strength between neurons can be adjusted adaptively according to the activities of neurons or the changes of the networks themselves [3–7]. This adaptive coupling is motivated by the phenomenon of synaptic plasticity [8,9]. Abbott *et al*. observed synaptic plasticity in neurophysiological networks, where the rate of signal propagation between neurons depends on their state [10]. Freeman *et al*. found that the circadian network is plastic and flexible, i.e., the synaptic coupling between neurons through the neurotransmitter GABA is plastic and their interaction strength is also highly dynamical [11].

The ability to adapt to changes in the coupling strength has attracted widespread attention from researchers [12–16] and has been widely applied in the field of complex networks, including the vascular network [17], the glymphatic network of the brain [18,19], osteocyte network formation [20], and in neural networks in the brain [21,22]. The renowned neurobiologist Cajal proposed that the changes in the coupling strength between two neurons should be related to learning. Juttner *et al*. studied a general adaptive learning rule with three parameters (strength of adaptivity, adaptivity offset, adaptivity shift) and simulated the learning paradigms based on peak-time-dependent plasticity, using the minimum model of Kuramoto phase oscillators [7]. Juttner *et al*. found that the nonadaptive models exhibit very simple dynamic behavior, while the nontrivial bifurcation structures collapse when the adaptation strength exceeds a critical threshold, resulting in more interesting and rich dynamic phenomena [7]. Huang *et al*. found that a simple adaptive law for coupling strength could induce global synchronization in weighted networks [23]. Wu *et al*. found that the resonance of adaptive coupling can reach a much larger value than that of fixed coupling, because the adaptive coupling can stimulate increasingly more elements to respond to external signals [5]. In addition, the synchronization of the whole system with the adaptive coupling is better than that with the fixed coupling, which was consistent with the results reported by Huang *et al.* [23]. Therefore, to improve functional robustness and synchronization in complex networks, such as brain networks, adaptive coupling should be the preferred mode of coupling above static coupling [21,24–26].

In addition to synchronization, entrainment is an important collective dynamical behavior in complex networks, especially in the field of circadian rhythms [27–29]. In mammals, the circadian rhythms are controlled by the suprachiasmatic nucleus (SCN) located in the brain [30]. The SCN is composed of approximately 20,000 neuronal oscillators, which are coupled through neurotransmitters to form a network, thereby outputting a unified periodic rhythm [31,32]. However, it is unclear how the SCN circadian rhythm is so robust and flexible. Gu *et al*. have conducted extensive research on both the SCN neuronal networks and neuronal characteristics to explain the collective behaviors of the SCN, but these studies were based on the assumption that the coupling strength between neuronal oscillators is fixed over time [33,34]. However, experimental evidence has shown that the SCN network is plastic and flexible, and the neural connections of the SCN vary over time at different time scales [35]. In addition, Freeman *et al*. found that the synaptic coupling between neurons through the neurotransmitter GABA is plastic, and their interaction strength is also highly dynamical [11]. Here, we are

*Contact author: gu_changgui@163.com

 ©2024 American Physical Society

focused on how the changes in coupling strength affect the collective behaviors of the SCN, such as entrainment.

Entrainment, as an important function of the SCN, refers to the ability of the SCN to entrain to the external cycle. Specifically, the minimum period of the external cycle that the SCN can entrain to is called the lower limit of entrainment (LLE), and the maximum period of the external cycle is called the upper limit of entrainment (ULE) [36,37]. The range between the LLE and the ULE is called the entrainment range, which is an indicator of the flexibility of the SCN to adapt to the external environmental changes [38]. The entrainment range varies from species to species. For example, a human can be entrained from 20.5 h to 29.0 h, a deer mouse can be entrained from 22.5 h to 25.1 h, and a southern flying squirrel can be entrained from 23.5 h to 24.9 h [31].

Generally speaking, the external signal of circadian entrainment is light [39]. In the SCN, not all the neuronal oscillators are sensitive to the light information [29]. According to the difference in sensitivity of neuronal oscillators to the light information, the SCN is divided into two subgroups, in which the neuronal oscillators in one subgroup are sensitive to the light information, which we call the ventrolateral (VL) subgroup, and the neuronal oscillators in the other subgroup are not sensitive to the light information, which we call the dorsomedial (DM) subgroup [39,40]. The VL and the DM synchronize their periods through a coupled pathway of the neurotransmitter GABA [41].

Because of the lack of specific rules for the variation of the coupling strength in the SCN, in this article, we take adaptive coupling to study its influence on the entrainment range of the SCN. The remainder of this article is arranged as follows. In Sec. II, a generalized Kuramoto model is introduced, which includes adaptive coupling. In Sec. III, the influence of the adaptive coupling on both the coupling strength within and between the VL and the DM, and the SCN entrainment range are systematically examined. In Sec. IV, the numerical simulation results in Sec. III are theoretically analyzed. Our results are summarized and discussed in Sec. V.

II. METHODS

The typical Kuramoto model can be applied to describe the neural network of the SCN [42]. It only considers the phase information of the neuronal oscillators and focuses on the interactions between different oscillatory neurons [43]. In this article, an extended Kuramoto model is introduced to mimic the SCN network exposed to an external periodic signal, where the coupling strength is adaptive [7,44]. In order to distinguish the VL and the DM, the SCN network composed of N neuronal oscillators is subdivided into two groups of neurons (VL and DM), and can be written as

$$\begin{aligned}
&\dot{\theta}_i = \frac{2\pi}{\tau} + \frac{1}{N}\sum_{j=1}^{N} g_{ij}\sin(\theta_j - \theta_i) + L\sin\left(\frac{2\pi}{T}t - \theta_i\right),\\
&i = 1, 2, \ldots, pN,\\
&\dot{\theta}_i = \frac{2\pi}{\tau} + \frac{1}{N}\sum_{j=1}^{N} g_{ij}\sin(\theta_j - \theta_i), \quad i = pN+1, \ldots, N,
\end{aligned} \tag{1}$$

where the overdot denotes differentiation with respect to time t, and the subscript i represents the ith neuronal oscillator. The variable θ_i is the phase of the ith neuronal oscillator in the absence of mutual interactions and external periodic signals. The parameters τ and N are the intrinsic period of the neuronal oscillator and the total number of neuronal oscillators in the SCN network, respectively. The neuronal oscillators i and j interact through a sine function. Note that an all-to-all coupling scheme is used here, as we do not investigate different network structures in this paper.

g_{ij} is the coupling strength between neuronal oscillators i and j. Adaptive coupling is applied by introducing a cosine function that is adaptable by an adaptation strength [7,45], and can be defined as

$$\dot{g}_{ij} = \epsilon(a + b\cos(\theta_i - \theta_j) - g_{ij}), \tag{2}$$

where $i \neq j$. The adaptive coupling strength g_{ij} increases at a rate of change related to the phase difference between the neuronal oscillators i and j. The coupling strength increases proportionatly to the synchronization difference in order to suppress the difference. The key parameter b is introduced to represent the adaptation strength, i.e., the impact level of interaction between two neuronal oscillators on the coupling strength. The parameter a is a constant that does not change with time, i.e., a fixed coupling strength without adaptive coupling rules ($b = 0$). The last term of g_{ij} ensures the boundedness of the coupling strengths. The time scale at which adaptation may occur is set by ϵ. Because $\cos(\theta_i - \theta_j) = \cos(\theta_j - \theta_i)$, the coupling strength g_{ij} is symmetric coupling, i.e., $g_{ij} = g_{ji}$.

The parameter p represents the ratio of the number of neuronal oscillators that can directly receive external periodic signals to the total number of neuronal oscillators in the SCN network. For simplicity, if the neuronal oscillator i is located in the VL subgroup, i.e., $0 < i \leqslant pN$, we assume that the neuronal oscillator receives external periodic signals. If the neuronal oscillator i is located in the DM subgroup, i.e., $pN < i \leqslant N$, we assume that the neuronal oscillator does not receive external periodic signals. $L\sin(\frac{2\pi}{T}t - \theta_i)$ is an external periodic signal, which in this article refers to the external light-dark cycle. The parameter L is the amplitude of the external periodic signal, which is the light sensitivity, and T is the period of the external light-dark cycle.

If the mean-square deviation (MSE) between the period T of the external light-dark cycle and the entrained periods T_i of the SCN neuronal oscillators was smaller than 10^{-5} h, we defined that the SCN was synchronized or entrained to the external cycle.

The details for the numerical simulations are presented as follows. The parameters were set as $\tau = 24$, $\epsilon = 0.2$, and $p = 0.50$ throughout the present article [7,42]. In the following sections, we will examine whether the entrainment range of the SCN is affected by the adaptation strength b, so the adaptation strength b was examined from 0 to 0.2. The fixed coupling strength a was set to 0.05, 0.10, and 0.15. Since there was no evidence to show whether the coupling effect is larger than the light effect or vice versa, the value of a was adjusted accordingly. When $a = 0.05$, the value of L was set to 0.03, 0.04, 0.05, 0.06, and 0.07. For $a = 0.10$, the value of L was

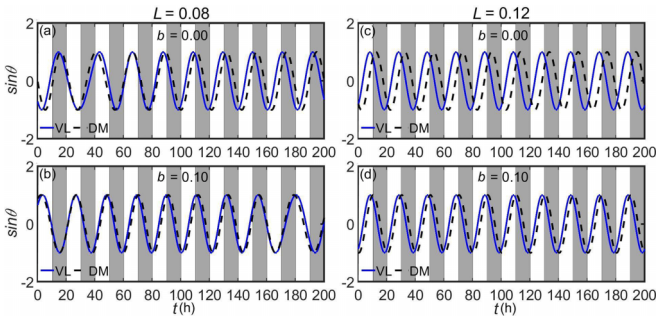

FIG. 1. The temporal evolutions of the two subgroups with typical adaptation strength b and light sensitivity L exposed to a 20 h external light-dark cycle. The value of light sensitivity is $L = 0.08$ in (a) and (b), and $L = 0.12$ in (c) and (d). The value of adaptation strength is $b = 0.00$ (a), (c) and $b = 0.10$ (b), (d). The fixed coupling strength $a = 0.10$ and the ratio $p = 0.50$. The grey regions and the white regions represent the night time and day time, respectively.

set as 0.06, 0.08, 0.10, 0.12, and 0.14. For $a = 0.15$, the value of L was set as 0.09, 0.12, 0.15, 0.18, and 0.21.

In the present article, the fourth-order Runge-Kutta method was applied with a time increment of 0.01 h for our numerical simulations. The initial 1 000 000 time steps were neglected in order to avoid the effect of transients, and the next 200 000 time steps were selected. The initial conditions of variable θ_i were selected randomly from a uniform distribution in the range from 0 to 2π for each neuronal oscillator. In the following sections, we take $N = 4$ as an example to show the results.

III. NUMERICAL RESULTS

A. The effect of the adaptive coupling on the phase of oscillators

Current experimental studies have shown that the intrinsic period of the SCN neuronal oscillators ranges from 22 h to 28 h [46]. Because of the flexibility of the Kuramoto model in non-24-hour external cycles, the simulated value of the entrainment range may be relatively large compared to the actual value. That is, the value of LLE may be smaller than 22 h, and the value of ULE may be larger than 28 h. We take the light-dark cycle exposed to 20 h as an example. When the fixed coupling strength a is 0.10, the influence of adaptation strength b on the temporal evolutions of the two subgroups with selected values of parameters L are shown in Fig. 1. When the light sensitivity L is 0.08 ($L < a$), whether $b = 0.00$ (a) or 0.10 (b), the period of the VL subgroup and the DM subgroup deviates considerably from the period of the external cycle. This means that the subgroups are both not entrained to the external 20 h cycle. When the light sensitivity L is 0.12 ($L > a$), if $b = 0.00$ (c), the VL and the DM oscillators have distinct periods and therefore the phase differences between the two subgroups are changing from cycle to cycle. Interestingly, if the value of b increases to 0.10 (d), each neuronal oscillator is entrained to the external cycle, which leads to a stable phase difference between the two subgroups. Therefore, it can be seen that the effect of b on the entrainment range is different between the cases of $L = 0.08$ and 0.12.

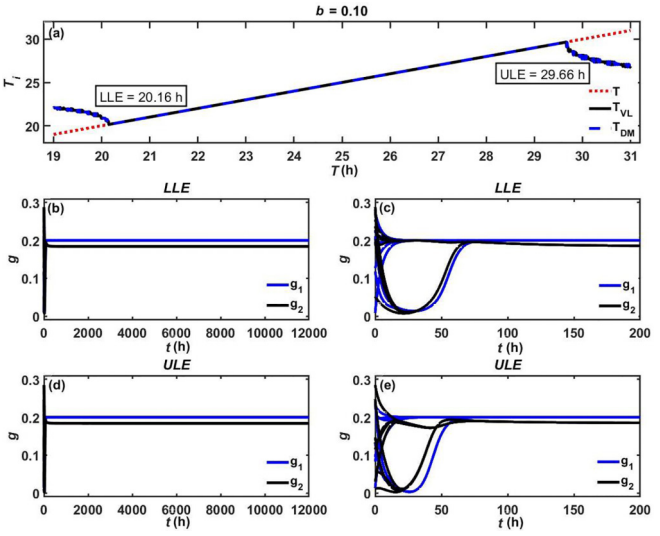

FIG. 2. The time evolutions of the coupling strength g at the LLE and the ULE. (a) The periods of the VL and the DM subgroups when the external period T ranges from 19.00 h to 31.00 h. (b) The time evolutions of the values of g at the LLE when time t ranges from 0 h to 12 000 h. (c) The time evolutions of the values of g at the LLE when time t ranges from 0 h to 200 h. (d) The time evolutions of the values of g at the ULE when time t ranges from 0 h to 12 000 h. (e) The time evolutions of the values of g at the ULE when time t ranges from 0 h to 200 h. The value of light sensitivity is $L = 0.10$. The fixed coupling strength $a = 0.10$ and the ratio $p = 0.50$.

B. The effect of adaptation strength

When the total number of neuronal oscillators $N = 4$ and the ratio $p = 0.50$, we assume that neuronal oscillators "1" and "2" are located in the VL subgroup, and neuronal oscillators "3" and "4" are located in the DM subgroup. From Eq. (2), it can be seen that g_{12} and g_{21} represent the coupling strength within the VL subgroup, g_{34} and g_{43} represent the coupling strength within the DM subgroup, and $g_{12} = g_{21} = g_{34} = g_{43}$. In the following, g_1 is applied to represent the coupling strength within the VL subgroup and the DM subgroup. g_{13}, g_{14}, g_{23}, g_{24}, g_{31}, g_{32}, g_{41}, and g_{42} represent the coupling strength between the VL subgroup and the DM subgroup, and $g_{13} = g_{14} = g_{23} = g_{24} = g_{31} = g_{32} = g_{41} = g_{42}$. In the following, g_2 is applied to represent the coupling strength between the VL subgroup and the DM subgroup.

In Fig. 2, we take $b = 0.10$ as an example to show that the period T_{VL} of the VL subgroup and the period T_{DM} of the DM subgroup when the external period T ranges from 19.00 h to 31.00 h (a), as well as the time evolutions of the values of g at the LLE [(b) and (c)] and the ULE [(d) and (e)]. From Fig. 2(a), we can observe that when 20.16 h $\leqslant T \leqslant$ 29.66 h, the values of T_{VL}, T_{DM}, and T are equal, i.e., the oscillators of the VL and the DM subgroups are all entrained by the external period T. We show the time evolutions of the coupling strength g for $T = 20.16$ h (LLE) in (b), where time t ranges from 0 h to 12 000 h. Note that for the sake of clarity, the coupling strength g_1 within the VL subgroup and the DM subgroup is represented in blue, and the coupling strength g_2 between the VL subgroup and the DM subgroup is represented in black. We can see that the values of g_1 and

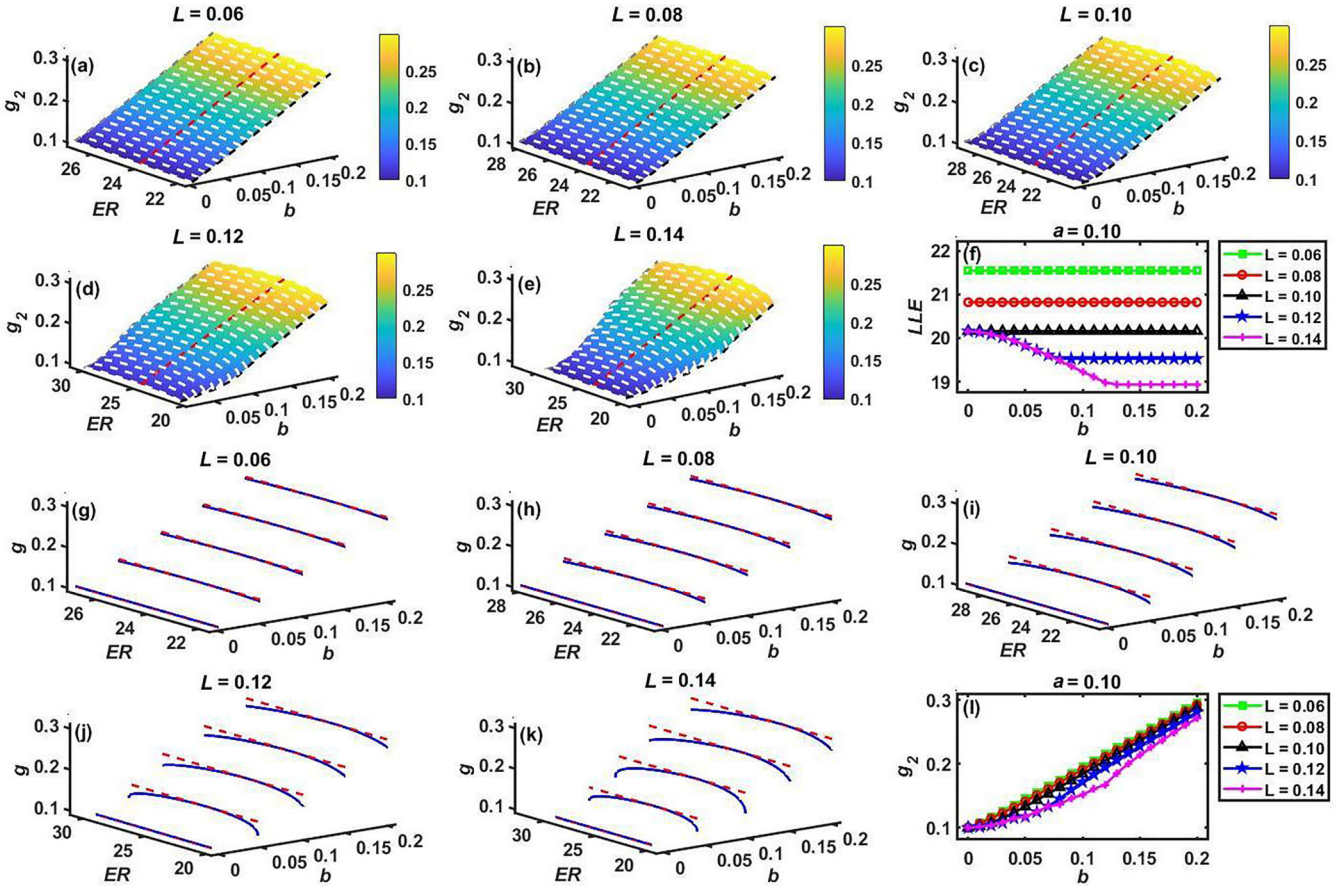

FIG. 3. The impact of the adaptation strength b on both the entrainment range and the coupling strength within and between the two subgroups. (a)–(e) The relationship between the entrainment range (ER) and b under five typical values of the light sensitivity L, as well as how the coupling strength between the two subgroups (g_2) varies with the increase of b within the entrainment range. Note that the red-dashed line represents the free running period (the period in constant darkness, FRP), the black-dashed line represents the LLE, the gray-dashed line represents the ULE, and the white-dashed line represents the variation trend of g_2 within the entrainment range of different values of b. (f) The effect of b on the LLE. (g)–(k) The variation trend of the coupling strength within and between the two subgroups within the entrainment range in five typical values of b. Note that the red dashed line and the blue solid line represent g_1 and g_2, respectively. (l) The effect of b on g_2. The number of neurons are $N = 4$. The fixed coupling strength $a = 0.10$ and the ratio $p = 0.50$.

g_2 tend to stabilize with time t. To avoid transient effects, we take the stabilized value of g as the coupling strength at the LLE. To better demonstrate the initial evolutions of the value of g, we show the time evolutions of the value of g in the first 200 h in Fig. 2(c), where the values of g at $t = 0$ h are given randomly. Accordingly, Figs. 2(d) and 2(e) correspond to Figs. 2(b) and 2(c), respectively, with the only difference being the time evolutions of the value of g at $T = 29.66$ h (ULE).

In Figs. 3(a)–3(e), we systematically examined the relationship between the entrainment range (ER) and the adaptation strength b under five typical values of the light sensitivity L, as well as how the coupling strength between the two subgroups (g_2) varies with the increase of b within the entrainment range [we do not show the coupling strength within the two subgroups (g_1)]. We observe that when $L = 0.06$, 0.08, and 0.10, the values of the LLE (black-dashed line) and the ULE (gray-dashed line) are both constant with the increase of b, i.e., the introduction of adaptive coupling has no effect on the entrainment range compared to the fixed coupling strength ($b = 0$). It is interesting that when $L = 0.12$ and 0.14, as b increases, the value of LLE decreases, while the value of ULE increases. That is, compared to the fixed coupling strength, the introduction of adaptive coupling widens the entrainment range. However, it should be noted that when the adaptation strength b reaches a certain threshold b_c, the entrainment range is no longer widened. Specifically, when $L = 0.12$, $b_c = 0.08$, and when $L = 0.14$, $b_c = 0.14$, indicating that as L increases, the threshold b_c also increases.

Considering that in the frequency domain, the LLE and the ULE are symmetric with respect to the intrinsic frequency, i.e., $\frac{2\pi}{LLE} - \frac{2\pi}{\tau} = \frac{2\pi}{\tau} - \frac{2\pi}{ULE}$, the entrainment range can be represented by the LLE. Note that, if the value of the LLE is smaller, the entrainment range is wider, and vice versa. We summarize the relationship between the entrainment range (represented by the LLE) and b under different light sensitivities L in Fig. 3(f). It is obvious that when there is no adaptive coupling ($b = 0$), the value of LLE decreases with the increase of L. When L reaches the threshold $L_c = 0.10$, continuing to increase L will no longer decrease the value of LLE, which has been verified in previous studies [29,42]. When adaptive coupling is introduced ($b > 0$), the value of LLE continues

to decrease when L is larger than 0.10, and as b increases, the threshold L_c increases. In summary, this indicates that the introduction of adaptive coupling can widen the entrainment range when L is large.

From Figs. 3(a)–3(e), it can be seen that as b increases, the coupling strength between the two subgroups within the entrainment range increases. In order to show more clearly how the coupling strength within and between the two subgroups varies within the entrainment range of a specific b, we select five typical values of b in Figs. 3(g)–3(k), namely 0.00, 0.05, 0.10, 0.15, and 0.20. It is obvious that when $b = 0$, regardless of the value of L, the values of g_1 and g_2 are constant and equal from the LLE to the ULE. As b increases, from the LLE to the ULE, the value of g_1 remains constant but the value of g_2 first increases and then decreases, and the maximum value is obtained at the external period $T = 24$ h and is equal to g_1. Note that the values of g_2 are equal at the LLE and the ULE. In short, within the entrainment range, the coupling strength within the two subgroups is constant, while the coupling strength between the two subgroups is symmetric about $T = 24$ h. As L increases, the difference between the value of g_2 and g_1 becomes larger at the LLE and the ULE. Since the value of g_1 remains constant and the value of g_2 is equal at the LLE and the ULE, in this article we can use the value of g_2 at the LLE to represent the magnitude of the coupling strength. Thus we summarize the relationship between the g_2 and b under different light sensitivities L in Fig. 3(l). Because of the difference between the value of g_2 at the LLE and the coupling strength is very small even if L increases, in some cases, we can assume that the coupling strength between the two subgroups does not change or changes very little within the entrainment range.

For comparison, the results are examined with the different fixed coupling strengths, i.e., $a = 0.05$ in Fig. S1 and $a = 0.15$ in Fig. S2 (see the Supplemental Material [47]), respectively. We observe that the numerical results shown in Figs. S1 and S2 are similar to Fig. 3. Based on Fig. 3 and Figs. S1 and S2, it can be concluded that when the light sensitivity L is small than the fixed coupling strength a, the existence of adaptive coupling has no effect on the entrainment range. However, when the light sensitivity L is larger than the fixed coupling strength a, the existence of adaptive coupling can widen the entrainment range.

In addition, we examine whether the number of neuronal oscillators N has an effect on the results. Without loss of generality, we considere the case of $N = 10$, 100, and 200, and the results are shown in Figs. S3, S4, and S5 (see the Supplemental Material [47]), respectively. We observe that the results are not affected by the number of neuronal oscillators. We also examine whether the main results are affected by the ratio p of the number of neuronal oscillators that can directly receive external periodic signals to the total number of neuronal oscillators in the SCN network [42,48]. Therefore, we investigate the case of $p = 0.25$ (Fig. S6) and $p = 0.75$ (Fig. S7) (see the Supplemental Material [47]), and the results are consistent with those shown in Fig. 3. Experimental studies have found that the intrinsic periods of the neuronal oscillators in the VL subgroup and the DM subgroup are different [49]. Considering that the neuronal oscillators in the DM subgroup run faster than those in the VL subgroup, the intrinsic period τ of the VL subgroup is set to 24.5 h and the DM subgroup is set to 23.5 h (see the Supplemental Material [47]). The results shown in Fig. S8 (within the Supplemental Material [47]) are qualitatively consistent with Fig. 3.

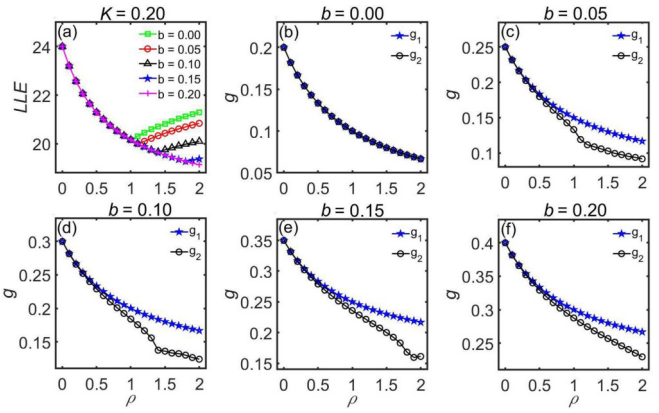

FIG. 4. The impact of the ratio between the light sensitivity and the fixed coupling strength ρ on both the LLE and the coupling strength within and between the two subgroups under five typical values of the adaptation strength b. (a) The relationship between the LLE and ρ under five typical values of b. The effect of ρ on the coupling strength within and between the two subgroups in the cases of (b) $b = 0.00$, (c) $b = 0.05$, (d) $b = 0.10$, (e) $b = 0.15$, and (f) $b = 0.20$, respectively. The number of neurons are $N = 4$. The parameter $K = 0.20$ and the ratio $p = 0.50$. Note that the coupling strength here is obtained at the LLE.

C. The effect of ratio between the light sensitivity and the fixed coupling strength

Considering that the relationship between the light sensitivity L and the fixed coupling strength a can affect the influence of adaptive coupling on the entrainment range, a key parameter ρ is introduced to represent the ratio between the light sensitivity and the fixed coupling strength, i.e., $\rho = \frac{L}{a}$. For comparison, another parameter $K = L + a$ is introduced to represent the sum of the light sensitivity and the fixed coupling strength, where K is set to 0.20. When the ratio $\rho = 1$, we obtain $L = a$; when the ratio $\rho < 1$, we obtain $L < a$; when the ratio $\rho > 1$, we obtain $L > a$.

Next, we further examine the effect of the ratio ρ between the light sensitivity and the fixed coupling strength on the entrainment range (represented by the LLE) in Fig. 4(a), where the ratio ρ ranges from 0 to 2. We can see that whether there is adaptive coupling or not, the relationship between the LLE and the ratio ρ is parabolic-like, meaning that as the ratio ρ increases, the value of LLE first monotonically decreases and then monotonically increases. Specifically, when the ratio ρ is smaller than 1, the value of b has no effect on the LLE, and the LLE monotonically decreases with the increase of the ratio ρ. When the ratio $\rho = 1$, the value of LLE is minimal in the case of $b = 0$, which means the maximum entrainment range is obtained. Continuing to increase the ratio ρ, when $b = 0$, the value of LLE increases, indicating that the entrainment range begins to narrow. However, when $b \neq 0$, the value of LLE continues to decrease, indicating that the entrainment range can continue to widen. In particular, when $b = 0.05$, 0.10,

0.15, and 0.20, the maximal entrainment ranges are obtained at ratios $\rho = 1.1$, $\rho = 1.4$, $\rho = 1.8$, and $\rho > 2$, respectively. In summary, when L is larger than a, the existence of adaptive coupling can widen the entrainment range.

Observing Figs. 4(b)–4(f), it can be seen that when $b = 0$, the values of g_1 and g_2 are equal and both decrease with the increase of ρ. When $b \neq 0$, as ρ increases, the values of g_1 and g_2 both decrease but $g_1 > g_2$. van Beurden *et al.*, estimated the coupling strength between and within neuronal subgroups in a two-community noise Kuramoto model [50]. They found a negative linear relationship between the coupling strength within subgroups and the coupling strength between subgroups. Although it is not possible to determine the specific magnitude relationship between the coupling strength within subgroups and the coupling strength between subgroups, the coupling strength within neuronal subgroups is larger than that between subgroups within the possible linear constraint range. In this article, the addition of adaptive coupling spontaneously leads to $g_1 > g_2$, which is similar to their findings. Moreover, we also verify the effect of $K = 0.10$ on the result in Fig. S9 (see the Supplemental Material [47]), and find that the result is qualitatively consistent with Fig. 4.

Corresponding to Figs. S3, S4, S5, S6, S7, and S8 (see the Supplemental Material [47]), we examine the number of neuronal oscillators $N = 10$, 100, and 200, the ratios $p = 0.25$ and 0.75, as well as the intrinsic period of the VL subgroup is 24.5 h and that of the DM subgroup is 23.5 h, as shown in Figs. S10, S11, S12, S13, S14, and S15 (see the Supplemental Material [47]). The results are consistent with those shown in Fig. 4.

IV. ANALYTICAL RESULTS

In this section, analyses are provided to explain the corresponding results of the numerical simulation. Because the results of $p = 0.25$, 0.50, and 0.75 are qualitatively consistent, we take $p = 0.50$ as an example. To simplify the analysis, we set the number of neuronal oscillators as $N = 4$, i.e., neuronal oscillators "1" and "2" are located in the VL subgroup, and neuronal oscillators "3" and "4" are located in the DM subgroup. Then, Eqs. (1) and (2) can be reduced to

$$\begin{aligned}
\dot{\theta}_1 &= \frac{2\pi}{\tau} + \frac{1}{4}\sum_{j=1}^{4} g_{1j}\sin(\theta_j - \theta_1) + L\sin\left(\frac{2\pi}{T}t - \theta_1\right),\\
\dot{\theta}_2 &= \frac{2\pi}{\tau} + \frac{1}{4}\sum_{j=1}^{4} g_{2j}\sin(\theta_j - \theta_2) + L\sin\left(\frac{2\pi}{T}t - \theta_2\right),\\
\dot{\theta}_3 &= \frac{2\pi}{\tau} + \frac{1}{4}\sum_{j=1}^{N} g_{3j}\sin(\theta_j - \theta_3),\\
\dot{\theta}_4 &= \frac{2\pi}{\tau} + \frac{1}{4}\sum_{j=1}^{N} g_{4j}\sin(\theta_j - \theta_4),\\
\dot{g}_{ij} &= \epsilon[a + b\cos(\theta_i - \theta_j) - g_{ij}], \quad i, j = 1, 2, 3, 4, \qquad (3)
\end{aligned}$$

where $i \neq j$.

When all the neuronal oscillators are entrained to the external cycle, the period between the neurons within the VL and the DM subgroups is the same and there is no phase difference, and we have $\theta_1 = \theta_2$, $\theta_3 = \theta_4$, and $\dot{\theta}_1 = \dot{\theta}_2 = \dot{\theta}_3 = \dot{\theta}_4 = \Omega$, where Ω is the angular frequency. The period between the VL neurons and the DM neurons is the same but there is a phase difference, so we assume that the phase difference between the VL neurons and the DM neurons is $\beta = \theta_1 - \theta_3 = \theta_1 - \theta_4 = \theta_2 - \theta_3 = \theta_2 - \theta_4$ and $\phi_i = \theta_i - \Omega t$. Because of the fact that the coupling strength is stabilized at a fixed value after adaptive rules, we assume that $\dot{g}_{ij} = 0$.

Since $\theta_1 = \theta_2$, $\theta_3 = \theta_4$, and $\cos(\theta_i - \theta_j) = \cos(\theta_j - \theta_i)$, we can get $g_{12} = g_{21} = g_{34} = g_{43}$, and $g_{13} = g_{14} = g_{23} = g_{24} = g_{31} = g_{32} = g_{41} = g_{42}$. In order to simplify Eq. (3), the coupling strength within the two subgroups is represented by g_1, i.e., $g_1 = g_{12} = g_{21} = g_{34} = g_{43}$, and the coupling strength between the two subgroups is represented by g_2, i.e., $g_2 = g_{13} = g_{14} = g_{23} = g_{24} = g_{31} = g_{32} = g_{41} = g_{42}$. Substituting them into Eq. (3), we obtain

$$\begin{aligned}
\Omega &= \frac{2\pi}{\tau} - \frac{1}{2}g_2\sin\beta - L\sin\phi_1,\\
\Omega &= \frac{2\pi}{\tau} + \frac{1}{2}g_2\sin\beta,\\
g_1 &= a + b,\\
g_2 &= a + b\cos\beta. \qquad (4)
\end{aligned}$$

Since the entrainment range can be expressed in terms of the LLE, and the value of the coupling strength can be expressed in terms of the value of the coupling strength at the LLE, we next explain the changing trend of coupling strength within and between the two subgroups, as well as the changing trend of the LLE, as the adaptation strength b increases under different light sensitivity L and fixed coupling strength a. Below, we will discuss it in two cases, i.e., $L < a$ and $L > a$.

From the last two lines of Eq. (4), it can be seen that as b increases, g_1 and g_2 both increases, indicating an increase in the coupling strength within and between the two subgroups. Because $0 < \cos\beta < 1$, $g_1 > g_2$ can be obtained, which means that the coupling strength within the two subgroups is larger than the coupling strength between the two subgroups. This also shows that the difference between the coupling strength within the two subgroups and the coupling strength between the two subgroups is caused by the phase difference β of the oscillators in different subgroups.

Note that LLE is equal to $\frac{2\pi}{\Omega_{\max}}$. When the light sensitivity is smaller than the fixed coupling strength, the phase difference β between the neuronal oscillators located in the two subgroups is very small, thus $\sin\beta \approx \beta$. Here, β is a very small positive value. By adding the first and second lines of Eq. (4), we obtain $\Omega_{\max} = \frac{2\pi}{\tau} - \frac{L}{2}\sin\phi_1$. Therefore, $\Omega_{\max}$ is a constant, which is independent of b.

Generally speaking, when the light sensitivity is larger than the coupling strength, $\Omega_{\max}$ depends on the slower oscillator with smaller Ω and $\sin\beta$ should be close to 1. Correspondingly, we obtain $\Omega_{\max} = \frac{2\pi}{\tau} + \frac{1}{2}g_2$. As g_2 increases with the increase of b, an increase in $\Omega_{\max}$ can be obtained.

Therefore, when the light sensitivity is larger than the fixed coupling strength, the adaptive coupling has no effect on the entrainment range. When the light sensitivity is smaller than the coupling strength, the adaptive coupling can widen the entrainment range. This is qualitatively consistent with the

numerical simulation results. In addition, with the increase of the adaptation strength b, the coupling strength within the two subgroups and between the two subgroups both increase, and $g_1 > g_2$, which is also qualitatively consistent with the numerical simulation results.

V. CONCLUSIONS AND DISCUSSION

The SCN is the main region that helps maintain the body's circadian rhythm, allowing endogenous rhythms to entrain to the external light-dark cycle [30]. The SCN is a heterogeneous neural network composed of approximately 20,000 oscillatory neurons, in which coupling plays an important role as the connecting edge of the network [31,32]. Previous studies have found that the entrainment range of the SCN depends on the coupling strength and the light sensitivity [33]. However, most previous studies have overlooked the plasticity of synaptic coupling between the neurons. The entrainment is partially attributable to the plasticity of the SCN network, and coupled plasticity has been proven to play an important role in memory and other advanced cognitive functions in the brain [11,35].

In this article, we considered the adaptive coupling based on the general Kuramoto model, where the interaction between neuronal oscillators is adaptively adjusted according to the phase difference of the neurons. We found that compared to a fixed coupling strength, when the light sensitivity is larger, the SCN networks with adaptive coupling strength show a broader range of external light-dark conditions to which they are able to entrain. This means that the adaptive coupling makes the circadian system more flexible to react to external influences. As a result, this flexibility may result in coping better with jet-lag or night shifts.

It was interesting to note that in the case of the adaptive coupling, the coupling strength within the two subgroups was spontaneously larger than that between the two subgroups, which is similar to the results speculated by van Beurden *et al*. within the possible linear constraint range [50]. Our research reveals the impact of adaptive coupling on the collective behavior of the SCN, and provides a possible explanation for the plasticity of coupling in the master clock network.

The results from this paper are generalizable to all systems that can be described by the Kuramoto model that has external forcing. For these systems, adaptive coupling results in a flexible system, where synchronization can occur more easily in a broader range of external conditions. There is evidence to suggest that the influence of light in nocturnal animals is higher than in diurnal (light-active) animals, including humans [51]. Therefore, the adaptive coupling may play a more important role in nocturnal species than in diurnal species.

In this article, we introduce adaptive coupling in the SCN networks. The influence of adaptive coupling on the entrainment range of the SCN is briefly studied, and the focus is on the adaptation strength. In our model, there is only a difference in the coupling strength within and between the two subgroups, meaning that there is no difference in the coupling strength between the two subgroups (without direction). Earlier study has found that the coupling strength from the VL subgroup to the DM subgroup is larger than that from the DM subgroup to the VL subgroup [52]. In future studies, we will consider the direction of the coupling strength in the adaptive rules to make our model more realistic, and investigate its impact on the ollective behavior of circadian rhythms.

ACKNOWLEDGMENTS

This work was supported by the National Natural Science Foundation of China (NSFC) under Grant No. 12275179 and the Shanghai Natural Science Foundation of China under Grant No. 21ZR1443900.

[1] X. F. Jiao, W. Y. Zhao, and J. D. Cao, Comput. Math. Methods Med. **2015**, 1 (2015).
[2] Y. B. Wu, Y. C. Li, and W. X. Li, Nonlinear Dyn. **96**, 2393 (2019).
[3] P. Seliger, S. C. Young, and L. S. Tsimring, Phys. Rev. E **65**, 041906 (2002).
[4] Y. L. Maistrenko, B. Lysyansky, C. Hauptmann, O. Burylko, and P. A. Tass, Phys. Rev. E **75**, 066207 (2007).
[5] D. Wu, S. Q. Zhu, X. Q. Luo, and L. Wu, Phys. Rev. E **84**, 021102 (2011).
[6] J. M. Li, W. Y. Zhang, and M. L. Chen, Comput. Math. Appl. **65**, 1775 (2013).
[7] B. Jüttner and E. A. Martens, Chaos **33**, 053106 (2023).
[8] W. Gerstner, R. Kempter, J. L. van Hemmen, and H. Wagner, Nature (London) **383**, 76 (1996).
[9] N. Caporale and Y. Dan, Annu. Rev. Neurosci. **31**, 25 (2008).
[10] M. Nouri, M. Jalilian, M. Hayati, and D. Abbott, IEEE Trans. Circuits Syst. II **65**, 804 (2018).
[11] G. M. Freeman, Jr., R. M. Krock, S. J. Aton, P. Thaben, and E. D. Herzog, Neuron **78**, 799 (2013).
[12] L. Lücken, O. V. Popovych, P. A. Tass, and S. Yanchuk, Phys. Rev. E **93**, 032210 (2016).
[13] R. Berner, J. Fialkowski, D. Kasatkin, V. Nekorkin, S. Yanchuk, and E. Schöll, Chaos **29**, 103134 (2019).
[14] R. Berner, J. Sawicki, and E. Schöll, Phys. Rev. Lett. **124**, 088301 (2020).
[15] T. Ruangkriengsin and M. A. Porter, arXiv:2203.12090.
[16] S. Thamizharasan, V. K. Chandrasekar, M. Senthilvelan, R. Berner, E. Schöll, and D. V. Senthilkumar, Phys. Rev. E **105**, 034312 (2022).
[17] E. A. Martens and K. Klemm, Front. Phys. **5**, 62 (2017).
[18] H. Mestre, T. Du, A. M. Sweeney, G. Liu, A. J. Samson, W. Peng, K. N. Mortensen, F. F. Stæger, P. A. R. Bork, L. Bashford, E. R. Toro, J. Tithof, D. H. Kelley, J. H. Thomas, P. G. Hjorth, E. A. Martens, and R. I. Mehta, Science **367**, eaax7171 (2020).
[19] T. Bohr, P. G. Hjorth, S. C. Holst, S. Hrabětová, V. Kiviniemi, T. Lilius, I. Lundgaard, K.-A. Mardal, E. A. Martens, Y. Mori, U. V. Nägerl, C. Nicholson, A. Tannenbaum, J. H. Thomas, J. Tithof, H. Benveniste, J. J. Iliff, D. G. Kelley, and M. Nedergaard, Science **25**, 104987 (2022).
[20] J. P. Taylor-King, D. Basanta, S. J. Chapman, and M. A. Porter, Phys. Rev. E **96**, 012301 (2017).
[21] J. Ito and K. Kaneko, Phys. Rev. Lett. **88**, 028701 (2001).

[22] J. M. Li, C. He, W. Y. Zhang, and M. L. Chen, Neurocomputing **219**, 144 (2017).
[23] D. Huang, Phys. Rev. E **74**, 046208 (2006).
[24] M. Chavez, M. Valencia, V. Navarro, V. Latora, and J. Martinerie, Phys. Rev. Lett. **104**, 118701 (2010).
[25] S. H. Strogatz, Physica D **143**, 1 (2000).
[26] M. A. Gkogkas, B. Jüttner, C. Kuehn, and E. A. Martens, Chaos **32**, 113120 (2022).
[27] C. G. Gu, H. J. Yang, J. H. Meijer, and J. H. T. Rohling, Phys. Rev. E **97**, 062215 (2018).
[28] M. Sujino, S. Koinuma, Y. Minami, and Y. Shigeyoshi, J. Biol. Rhythms **36**, 410 (2021).
[29] W. X. Zheng, C. G. Gu, H. J. Yang, and J. H. T. Rohling, Phys. Rev. E **105**, 014314 (2022).
[30] J. S. Takahashi, Nat. Rev. Genet. **18**, 164 (2017).
[31] R. Refinetti, *Circadian Physiology* (CRC Press, Boca Raton, FL, 2006).
[32] M. H. Hastings, E. S. Maywood, and M. Brancaccio, Nat. Rev. Neurosci. **19**, 453 (2018).
[33] C. G. Gu, H. J. Yang, and M. Wang, Commun. Theor. Phys. **70**, 771 (2018).
[34] C. G. Gu, P. Wang, and H. J. Yang, Chin. Phys. B **28**, 018701 (2019).
[35] J. X. Zhou, H. L. Wang, and R. Ouyang, Chaos **32**, 023101 (2022).
[36] R. Refinetti, Lab. Anim. **33**, 54 (2004).
[37] W. X. Zheng, C. G. Gu, H. J. Yang, and J. H. T. Rohling, Nonlinear Dyn. **111**, 12625 (2023).
[38] C. G. Gu, H. J. Yang, and Z. Y. Ruan, Phys. Rev. E **95**, 042409 (2017).
[39] Y. N. Li and I. P. Androulakis, Sci. Rep. **11**, 17929 (2021).
[40] D. K. Welsh, J. S. Takahashi, and S. A. Kay, Annu. Rev. Physiol. **72**, 551 (2010).
[41] E. D. Herzog, T. Hermanstyne, N. J. Smyllie, and M. H. Hastings, Cold Spring Harbor Perspect. Biol. **9**, a027706 (2017).
[42] W. X. Zheng, C. G. Gu, Y. Xu, and H. J. Yang, Chaos, Solitons Fractals **175**, 114051 (2023).
[43] C. G. Gu, Y. Zhang, W. X. Zheng, H. Y. Wang, H. J. Yang, and M. Wang, Int. J. Mod. Phys. C **34**, 2350050 (2023).
[44] X. F. Jiao and R. B. Wang, Appl. Phys. Lett. **88**, 203901 (2006).
[45] R. Wang and X. F. Jiao, Neurocomputing **69**, 778 (2006).
[46] S. Honma, W. Nakamura, T. Shirakawa, and K. Honma, Neurosci. Lett. **358**, 173 (2004).
[47] See Supplemental Material at http://link.aps.org/supplemental/10.1103/PhysRevE.110.034212 for examining the effects of the fixed coupling strengths, the number of neuronal oscillators, ratio, and the intrinsic period on the numerical simulation results.
[48] H. S. Lee, J. L. Nelms, M. Nguyen, R. Silver, and M. N. Lehman, Nat. Neurosci. **6**, 111 (2003).
[49] T. Noguchi, K. Watanabe, A. Ogura, and S. Yamaoka, Eur. J. Neurosci. **20**, 3199 (2004).
[50] A. W. van Beurden, J. M. Meylahn, S. Achterhof, R. Buijink, A. O. Engberink, S. Michel, J. H. Meijer, and J. H. T. Rohling, J. Biol. Rhythms **38**, 461 (2023).
[51] C. M. Novak, J. C. Ehlen, and H. E. Albers, Biol. Rhythm Res. **39**, 291 (2008).
[52] J. H. Rohling, H. T. van der Leest, S. Michel, M. J. Vansteensel, and J. H. Meijer, PLoS ONE **6**, e25437 (2011).